

Effects of electrophoretic deposition conditions on the formation of colloidal crystalline/amorphous arrays of SiO₂ particles.

Naoki Tarutani¹, Kenta Kawaguchi¹, Kiyofumi Katagiri¹, Kei Inumaru¹

¹ Graduate School of Advanced Science and Engineering, Hiroshima University, 1-4-1 Kagamiyama, Higashi-Hiroshima 739-8527, Japan

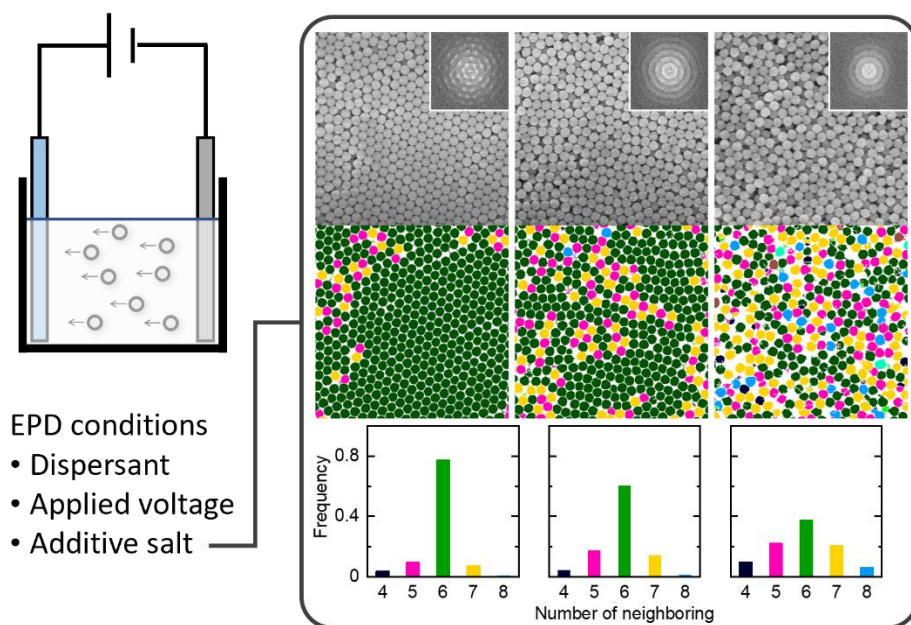
Corresponding author

Correspondence to Naoki Tarutani, Graduate School of Advanced Science and Engineering, Hiroshima University, 1-4-1 Kagamiyama, Higashi-Hiroshima 739-8527, Japan. E-mail: n-tarutani@hiroshima-u.ac.jp

Abstract

The ordering of monodispersed nano- and micro-scale particles has unique properties, such as selective light scattering, which are controlled by the degree of ordering. In structurally colored materials, particle arrays that have long-range-order (colloidal crystalline arrays) can exhibit vivid and illumination-angle-dependent color. In contrast, short-range-ordered arrays (colloidal amorphous arrays) exhibit matte and illumination-angle-independent color. We prepared SiO₂ particle arrays with controlled ordering via electrophoretic deposition. Dispersant organic solvents determined the formation of uniform arrays, the applied voltage had minor effects on the ordering, and an additive salt solution significantly changed the structures from colloidal crystalline arrays to colloidal amorphous arrays. Controlling these structures will be important for applications of structurally colored materials as novel colorants, such as color-controllable pigments.

Graphical Abstract



Keywords

electrophoretic deposition, structurally colored materials, colloidal crystalline arrays, colloidal amorphous arrays

Highlights

- Chemically stable SiO_2 particles allowed to investigate the effect of various electrophoretic deposition conditions.
- Organic solvent dispersants having moderate dielectric constant enabled uniform particle arrays.
- The applied voltage had minor effects while additive KCl solutions significantly changed array structures.

Introduction

Arrays of particles and pores at the nanometer/micrometer scale often yield functional materials. For example, nanoscale metal particle arrays have plasmonic resonances[1, 2], and sub-micrometer and micrometer-scale particles/pores arrays can control light[3, 4] and heat[5, 6]. Arrays of sub-micrometer particles are structurally colored materials and have been used as novel pigments. The physical origin of structurally colored materials is the interaction, such as diffraction, scattering and interfering, between visible light and fine structures of the array.[7] Assemblies of monodispersed spherical particles are versatile and reproducible ways to prepare materials exhibiting desired specific colors.[8–11] Long-range-ordered arrays (colloidal crystalline arrays) have been extensively investigated as structurally colored materials. The color is controlled by tuning the particle diameter, refractive index, and ordering.[12, 13] Characteristically, the color of colloidal crystalline arrays depends on the viewing angle. Therefore, they may be limited to decorative applications, such as jewelry, and not be applicable to others, such as paint for traffic signs. In contrast, short-range-ordered arrays (colloidal amorphous arrays) are structurally colored materials with angle-independent matte colors, non-iridescence color.[14] Hence, controlling the structures between colloidal crystalline and colloidal amorphous arrays enables a wide range of structurally colored materials for many applications.

Colloidal crystalline/amorphous arrays have been prepared via various methods, such as solvent evaporation,[15, 16] thermal-assisted processes,[17] centrifugation,[18, 19] drop-casting,[20] and spray-coating.[21, 22] However, these methods make it difficult to coat large surfaces quickly and to treat complex shapes. Alternatively, electrophoretic deposition (EPD) is a powerful, economical, and energy-efficient technique that can be used to deposit fine particles on large and complex surfaces.[23, 24] Our group has developed a EPD method to produce colloidal crystalline/colloidal amorphous array coatings.[25–27] Suspensions of monodisperse, spherical SiO₂ particles are used as starting materials. Films with controlled thicknesses have been prepared and exhibit bright structural colors, depending on the particle diameters.[25] Colloidal crystalline/amorphous arrays depend on the electrophoretic voltage[25] and the pH of the EPD sol[26]. However, those studies focused on specific rather than systematic conditions. Various EPD conditions, such as Zeta potential, solution conductivity, viscosity, particle stability against aggregation and applied voltage, significantly affect deposition kinetics[28]. Therefore, a systematic investigation is essential to control formation of colloidal crystalline/amorphous arrays. In addition, facing configuration of working and counter substrate electrodes will realize one directional electric field and simplify the kinetics of particles during EPD rather than the configuration of substrate working electrode with spiral counter electrode employed in the previous study for a homogeneous electric field from all directions. Although Uchikoshi *et al.* have reported a systematic investigation for polystyrene particles, the selection of the organic solvent was limited because polystyrene regrettably dissolves in various types

of organic solvents such as tetrahydrofuran.[29] Therefore, a systematic investigation of EPD using chemically stable particles is necessary to control the array structures.

Here, we used EPD of monodispersed SiO₂ particles and investigated the effects of the organic dispersant, the applied voltage, and additives on the formation of colloidal crystalline/amorphous arrays. SiO₂ is chemically stable in a wide variety of organic dispersants, such as ethanol, tetrahydrofuran, and acetonitrile, which produce significant effects on the EPD kinetics. The applied voltage was a minor effect over the range of 5–30 V cm⁻¹. A KCl aqueous solution was used as an additive that changed the structures from colloidal crystalline arrays to colloidal amorphous arrays. Overall, control of the SiO₂ particle array structures will be important for their use as color-controllable pigments.

Experimental

Chemicals

Monodisperse 200-nm SiO₂ spherical particles were obtained from Fuji Chemical Co., Ltd (Japan). Hydrogen peroxide solution (H₂O₂ aq., 30 wt.%) was purchased from Junsei Chemical Co., Ltd (Japan). Ammonium hydroxide solution (NH₄OH aq., 28 wt.%), ethanol (EtOH, 99.5%), 2-propanol (≥99.7%), ethylene glycol (EG, ≥98%), tetrahydrofuran (THF, 99.5%), dimethyl sulfoxide (DMSO, 99%), and propylene carbonate (PC, ≥98%) were obtained from Nacalai Tesque, Inc (Japan). Acetonitrile (ACN, 99.5%) was purchased from Kishida Chemical Co., Ltd. (Japan). Potassium chloride was purchased from FUJIFILM Wako Pure Chemical Corp. (Japan). All reagents were used as received without further purification. Ultrapure water (resistivity 18.2 MΩ·cm) from a Millipore Milli-Q system (Merck Millipore, USA) was used in all experiments.

Preparation of EPD films of SiO₂ arrays under various conditions

SiO₂ particles (1.4 g) were added to a H₂O/NH₄OH (5.4 mL/0.25 mL) solution and ultrasonicated for 1 h. Then, 80.75 mL of an organic solvent dispersant (EtOH, EG, THF, DMSO, PC, or ACN) was added to the suspension and ultrasonicated for 1 h. Subsequently, 10 μL of an aqueous KCl solution (0, 0.1, 0.25, or 0.35 mol L⁻¹) was added and the resultant suspension was used as the EPD sol. Indium tin oxide (ITO)-coated glass substrates (15-mm×40-mm) were used as working electrodes. Initially, the ITO-coated glass substrates were immersed in cleaning solution (H₂O:H₂O₂ aq.:NH₄OH aq., 5:1:1 by volume) at 60 °C for 30 min in a water bath to remove residual organic materials, followed by rinsing in deionized water. A 15-mm×40-mm stainless-steel plate (SUS430) was used as the counter electrode. The working and counter electrodes were immersed 10 mm apart in the EPD sol using home-made square shape cell. The EPD films were prepared on the anode ITO-coated glass substrate with a specific voltage (5–30 V cm⁻¹) and duration time (5 V cm⁻¹ for 30 min, 10 V cm⁻¹ for 15 min, 20 V cm⁻¹ for 7.5 min,

and 30 V cm⁻¹ for 5 min), using a potentiostat (SP-300, BioLogic Sciences Instruments). After the electrophoresis, the substrates were withdrawn from the solutions at a rate of 2 mm s⁻¹ and dried at ambient temperature. Each sample was labeled according to the dispersant, applied voltage, and KCl concentration (for example, EtOH-5V-0.1M).

Characterization

A field-emission scanning electron microscope (SEM; S-4800, Hitachi, Japan) was used to image the ordering of the SiO₂ particles. Fast Fourier transform (FFT) images and Voronoi diagrams were obtained from the SEM images using Fiji ImageJ v1.53p. Reflectance spectra were acquired with an ultraviolet-visible spectrometer (V-670, JASCO, Japan), equipped with an absolute reflectance measurement unit (ARMN-735). The detection angle was varied over the range 20–50°. The amount of electrical charge, Q , passed through the solution was recorded with a potentiostat (SP-300, BioLogic Sciences Instruments, France).

Results and discussion

Effect of dispersant on the EPD behavior of SiO₂ particles

The SiO₂ particles had negatively charged surfaces in the NH₄OH-containing solution because of their low isoelectric point (~2), and were thus electrophoretically deposited onto the ITO-coated glass anode.[25] Water-miscible organic solvents were selected to investigate the effect of dispersant on EPD film formation. Figure 1a shows the amount of electric charge, Q , passed during the deposition. It increased linearly with EPD duration time for all the samples, which indicated that the SiO₂ particles were deposited on the ITO-coated glass. The final Q value varied with the dispersant and increased with the dielectric constant (Figure 1b). Considering the electrophoretic mobility of particles given by Helmholtz–Smoluchowski equation:[28, 30] $\mu = \epsilon\epsilon_0\zeta/3\eta$, where μ , ϵ , ϵ_0 , ζ , and η are electrophoretic mobility, dielectric constant of media, dielectric constant of vacuum, zeta potential, and viscosity of media. The μ will increase with increasing the ϵ , which results increasing number of charged particle reaching the electrode in unit time and large Q value. Figure 2 shows SEM images of SiO₂ particle samples prepared with different organic dispersants. The EtOH-5V-0M sample formed a uniform flat film with a colloidal crystalline array [Figure 2(a)]. The THF-5V-0M, ACN-5V-0M, and PC-5V-0M samples exhibited inhomogeneous agglomerations with short-range-ordering (colloidal amorphous arrays). SiO₂ particles were scarcely deposited in PC-5V-0M and DMSO-5V-0M samples. Power[31] reported that EPD films of β -alumina were formed when the solvent had a dielectric constant in the range of 12–25. It was discussed that low-dielectric-constant dispersants had insufficient power to dissociate ions from the solid surface into liquid to give surface charge.[31, 32] In this study, the inhomogeneous short-range-ordered SiO₂ particle array formed as a

result of relatively low surface charge. Whereas, high-dielectric-constant dispersants reduced the double layer thickness and, consequently, the electrophoretic mobility, which resulted in poor deposition. Hence, by having a moderate dielectric constant, EtOH was the most suitable solvent for the synthesis of the EPD films composed of SiO₂ particles.

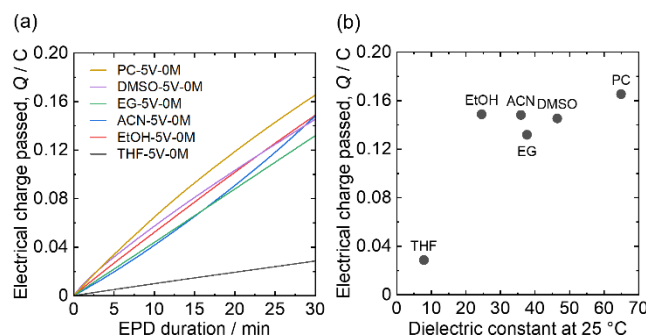


Figure 1. (a) Duration-dependent increases in electrical charge, Q , passed during electrophoretic deposition using THF, EtOH, ACN, EG, DMSO, and PC dispersants without KCl solution. (b) Relationship between 30-min cumulative Q values and dielectric constants at 25 °C for each dispersant.[33]

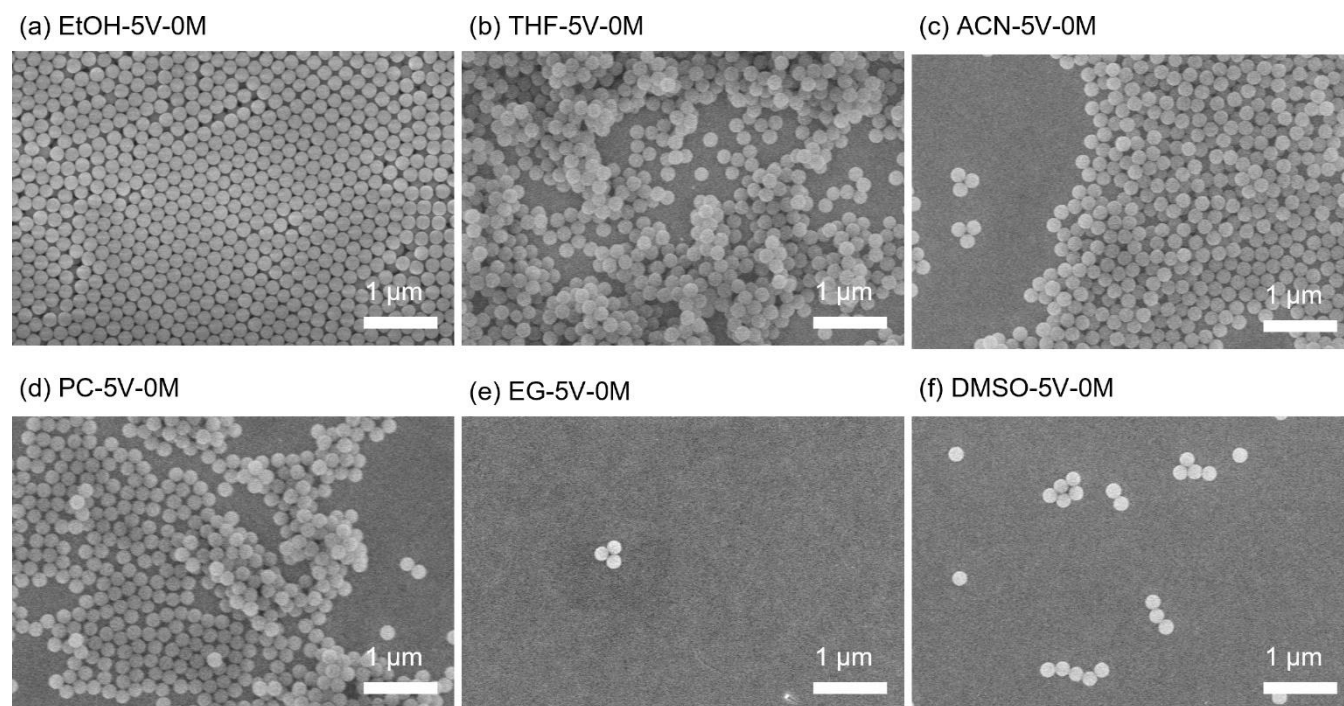


Figure 2. SEM images of (a) EtOH-5V-0M, (b) THF-5V-0M, (c) ACN-5V-0M, (d) PC-5V-0M, (e) EG-5V-0M, and (f) DMSO-5V-0M.

Effect of applied voltage on the EPD behavior of SiO₂ particles

The applied voltage was varied over 5–30 V cm⁻¹ in EtOH. EPD durations were set as noted above. To obtain comparable films, EPD durations decreased proportionately with increasing applied voltage so that the deposition amount becomes identical between the samples.[34, 35] All these samples formed uniform flat films of well-ordered arrays at 5–30 V cm⁻¹ in EtOH [upper panels in Figure 3(a-d)]. Corresponding FFT images revealed sharp hexagonal spots [lower panels in Figure 3(a-d)],

which verified well-ordered colloidal crystalline arrays. A Voronoi diagram is a computational geometry analysis [36, 37], which has been applied to colloidal array materials.[38, 39] As shown in the middle panels of Figure 3(a-d), the major array component was six-fold Voronoi polygons. Four-, five-, seven-, and eight-fold polygons were observed at domain boundaries, indicating disordered arrangements. The distributions of the number of neighboring are plotted in Figure 3(e) for approximately 3000 polygons. The relative fractions (0.68–0.77) of six-fold polygons were comparable for all these systems, which indicated that the domain size of the well-ordered SiO_2 particle array were comparable in all the samples. As reported previously,[25] electrophoretic mobility under low applied voltages was low enough to allow particle rearrangements to form close-packed colloidal crystalline arrays before deposition of the next layer. Colloidal amorphous arrays will form under high applied voltages because fast EPD will disrupt particle rearrangement, analogous to the mechanism of colloidal amorphous array formation via spray-coating.[40] Here, however, the effects of applied voltage on the particle arrangements were minor over the range $5\text{--}30\text{ V cm}^{-1}$.

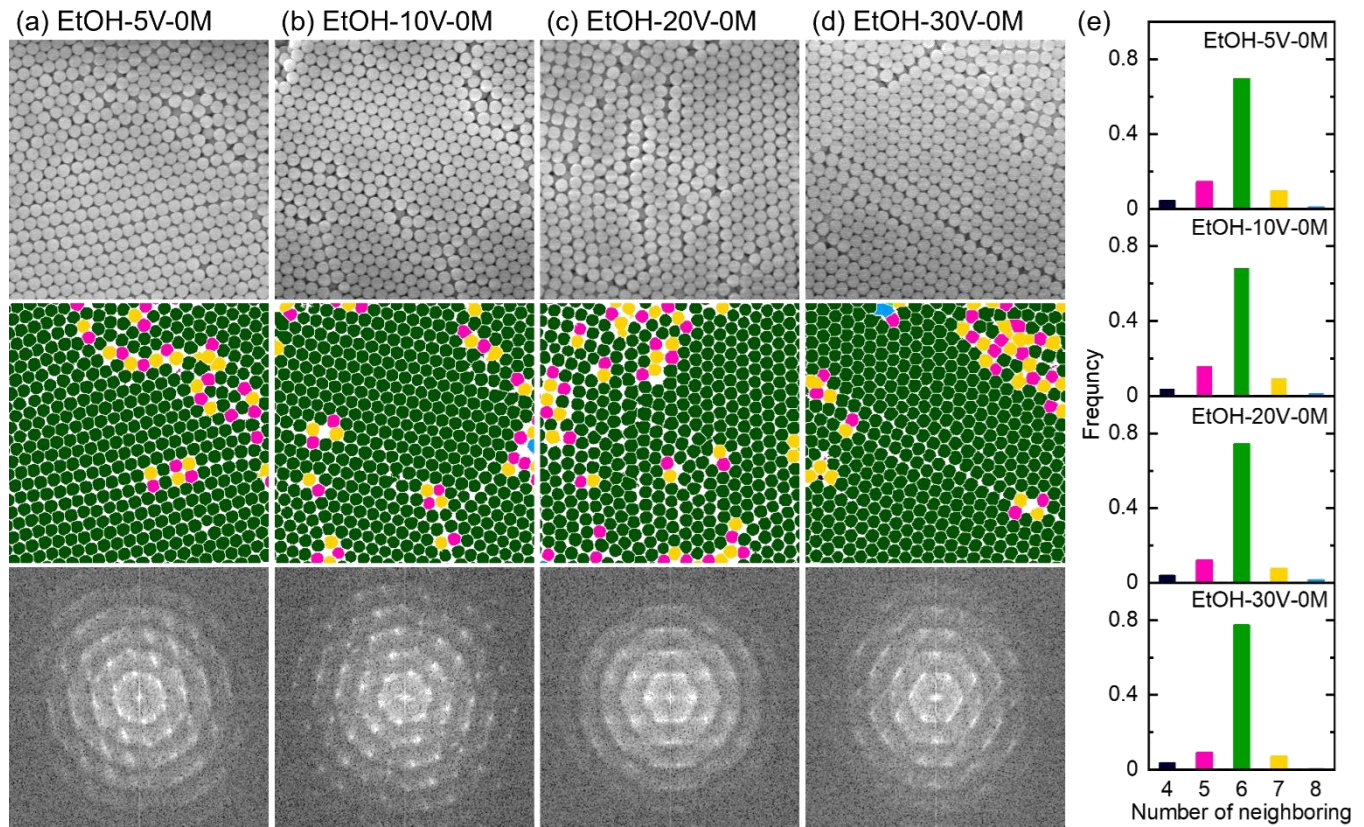


Figure 3. SEM images (upper panels), Voronoi diagrams (middle panels), and FFT images (lower panels) of (a) EtOH-5V-0M, (b) EtOH-10V-0M, (c) EtOH-20V-0M, and (d) EtOH-30V-0M. Four-, five-, six-, seven-, and eight-fold Voronoi polygons are shown in black, pink, green, yellow, and light-blue, respectively. (e) Distributions of the number of neighboring Voronoi polygons for EtOH-5V-0M, EtOH-10V-0M, EtOH-20V-0M, and EtOH-30V-0M (~3000 polygons counted).

Effect of KCl additive on the EPD behavior of SiO₂ particles

KCl was used to investigate additive effects on array formation. Figure 4 shows SEM images, Voronoi diagrams, FFT images, and distributions of the number of neighbors. When the concentration of KCl was increased in the additive solution, the particle arrays changed from colloidal crystalline arrays to colloidal amorphous arrays [upper panels in Figure 4(a-d)]. Corresponding FFT images changed from the sharp hexagonal spots of colloidal crystalline arrays to the blurred ring patterns of colloidal amorphous arrays. In the Voronoi diagrams, the EtOH-5V-0M mainly had six-fold polygons. Whereas, EtOH-5V-0.1M had non-negligible amounts of five- and seven-fold polygons, and the six-fold domains were smaller relative to those in EtOH-5V-0M. Further increases in KCl, such as for EtOH-5V-0.25M and EtOH-5V-0.35M, further decreased the number of six-fold polygons and collapsed their domains. Figure 4(e) shows that the relative fraction of six-fold polygons decreased from 0.77 (EtOH-5V-0M) to 0.60 (EtOH-5V-0.1M), 0.37 (EtOH-5V-0.25M), and 0.37 (EtOH-5V-0.35M) with increasing KCl concentrations in the additive solution.

Reflection spectra were acquired to characterize the entire areas of the samples. The incident angle was 0° relative to the films and the detection angle was varied over the range 20–50° [Figure 5(a)]. EtOH-5V-0M exhibited a sharp reflection peak at 420 nm [Figure 5(b)], which blue-shifted with increasing detection angle. This is a feature of colloidal crystalline arrays.[41] EtOH-5V-0.35M exhibited angle-independent reflection spectra [Figure 5(c)], which is a feature of colloidal amorphous arrays.[42, 43] Figure 5(d) shows detection-angle-dependent changes in the reflection peaks. The EtOH-5V-0M and EtOH-5V-0.1M were colloidal crystalline arrays and the EtOH-5V-0.25M and EtOH-5V-0.35M were colloidal amorphous arrays considering the angle dependent change of peak wavelength. The data were consistent with the SEM images. This implies that the observed structures occurred throughout the entire area of each film, considering the reflection detection area on the sample as large as 10 mm square.

In summary, the addition of the KCl solution significantly contributed to the arrangement of the SiO₂ particles. Increasing the ion concentrations reduced the thickness of the electrical double layer of the particles,[44] which decreased repulsions between the particles and retarded their rearrangement to form close-packed colloidal crystal arrays. Salt concentrations have been reported to affect particle arrangements not only during drying but also during wet conditions.[45] As a result, randomly agglomerated SiO₂ particle arrays were electrophoretic deposited and colloidal amorphous arrays were formed.

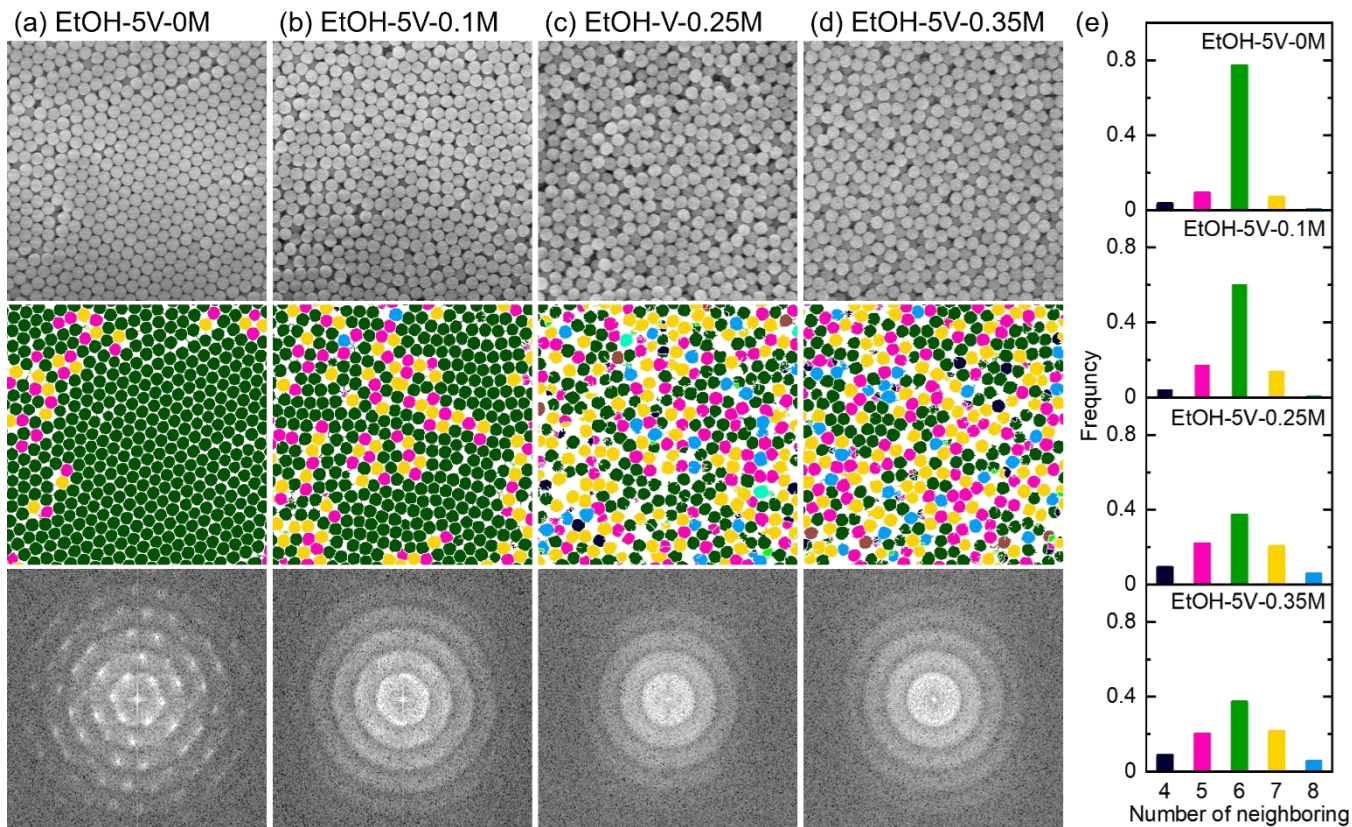


Figure 4. SEM images (upper panels), Voronoi diagrams (middle panels), and FFT images (lower panels) of (a) EtOH-5V-0M, (b) EtOH-5V-0.1M, (c) EtOH-5V-0.25M, and (d) EtOH-5V-0.35M. Four-, five-, six-, seven-, and eight-fold Voronoi polygons are shown as black, pink, green, yellow, and light-blue, respectively. (e) Distributions of the number of neighboring Voronoi polygons for EtOH-5V-0M, EtOH-5V-0.1M, EtOH-5V-0.25M, and EtOH-5V-0.35M (~3000 polygons counted).

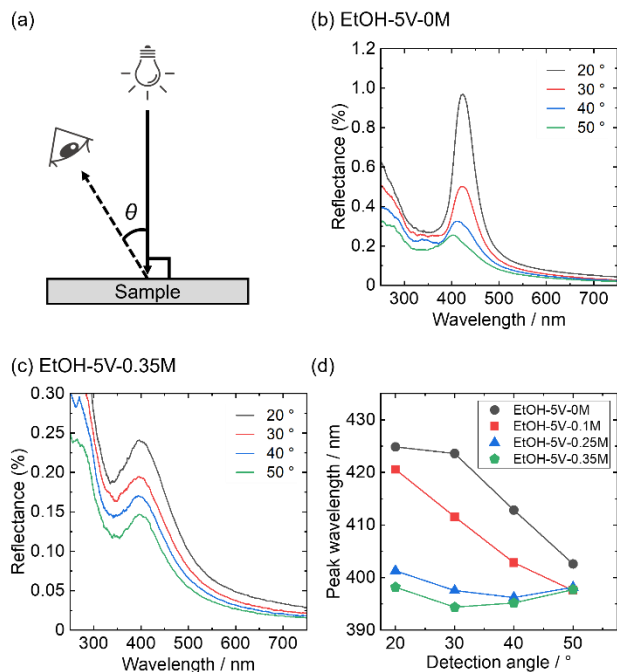


Figure 5. (a) Schematic of incident and detection angles for reflectance measurements. Reflectance spectra of (b) EtOH-5V-0M and (c) EtOH-5V-0.35M acquired with detection angles over the range 20–50°. (d) Detection-angle-dependence of changes

in the peak reflectance wavelength of EtOH-5V-0M (black circle), EtOH-5V-0.1M (red square), EtOH-5V-0.25M (blue triangle), and EtOH-5V-0.35M (green pentagon).

Conclusions

SiO₂ particle arrays were prepared via EPD using various organic solvent dispersants, which significantly affected the depositions. Ethanol was adequate because of its moderate dielectric constant. Applied voltages over the range 5–30 V cm⁻¹ had minor effects on the particle arrangements, where colloidal crystalline arrays formed in all cases without KCl solution. In contrast, additive KCl salt solutions had strong effects on particle arrangements, and essentially controlled the transition between colloidal crystalline and colloidal amorphous arrays. The reflectance spectra indicated that such colloidal crystalline or amorphous arrays formed throughout the entire areas of the deposited films.

ACKNOWLEDGMENTS

This work was partially supported by JSPS KAKENHI Grant Number JP18K19132, JP20H02439 and JP20K15368, MEXT Leading Initiative for Excellent Young Researchers, JSPS Core-to-Core Program, International Network on Polyoxometalate Science at Hiroshima University, the Cooperative Research Program of Institute for Catalysis, Hokkaido University (Grant numbers 20B1016 and 21A1007), the facilities of the Institute of Materials and Systems for Sustainability, Nagoya University, Iketani Science and Technology Foundation, and the Takahashi Industrial and Economic Research Foundation. We thank Edanz (<https://jp.edanz.com/ac>) for editing a draft of this manuscript.

REFERENCES

1. Gao B, Arya G, Tao AR (2012) Self-orienting nanocubes for the assembly of plasmonic nanojunctions. *Nat Nanotechnol* 7:433–437. <https://doi.org/10.1038/nnano.2012.83>
2. Murray WA, Barnes WL (2007) Plasmonic materials. *Adv Mater* 19:3771–3782. <https://doi.org/10.1002/adma.200700678>
3. Talapin D V., Lee J-S, Kovalenko M V., Shevchenko E V. (2010) Prospects of Colloidal Nanocrystals for Electronic and Optoelectronic Applications. *Chem Rev* 110:389–458. <https://doi.org/10.1021/cr900137k>
4. Lederer F, Stegeman GI, Christodoulides DN, et al (2008) Discrete solitons in optics. *Phys Rep* 463:1–126. <https://doi.org/10.1016/j.physrep.2008.04.004>
5. Anufriev R, Ramiere A, Maire J, Nomura M (2017) Heat guiding and focusing using ballistic phonon transport in phononic nanostructures. *Nat Commun* 8:1–8. <https://doi.org/10.1038/ncomms15505>
6. Tang J, Wang HT, Lee DH, et al (2010) Holey silicon as an efficient thermoelectric material. *Nano Lett* 10:4279–4283. <https://doi.org/10.1021/nl102931z>
7. Kinoshita S, Yoshioka S, Miyazaki J (2008) Physics of structural colors. *Reports Prog Phys* 71:076401. <https://doi.org/10.1088/0034-4885/71/7/076401>
8. Takeoka Y (2012) Angle-independent structural coloured amorphous arrays. *J Mater Chem* 22:23299–23309. <https://doi.org/10.1039/c2jm33643j>
9. Fudouzi H, Xia Y (2003) Colloidal crystals with tunable colors and their use as photonic papers. *Langmuir* 19:9653–9660. <https://doi.org/10.1021/la034918q>
10. Shang G, Maiwald L, Renner H, et al (2018) Photonic glass for high contrast structural color. *Sci Rep* 8:1–9. <https://doi.org/10.1038/s41598-018-26119-8>
11. Kohri M (2019) Artificial melanin particles: new building blocks for biomimetic structural coloration. *Polym J* 51:1127–1135. <https://doi.org/10.1038/s41428-019-0231-2>
12. Xia Y, Gates B, Yin Y, Lu Y (2000) Monodispersed colloidal spheres: Old materials with new applications. *Adv Mater* 12:693–713. [https://doi.org/10.1002/\(SICI\)1521-4095\(200005\)12:10<693::AID-ADMA693>3.0.CO;2-J](https://doi.org/10.1002/(SICI)1521-4095(200005)12:10<693::AID-ADMA693>3.0.CO;2-J)
13. Zhao Y, Xie Z, Gu H, et al (2012) Bio-inspired variable structural color materials. *Chem Soc Rev* 41:3297–3317. <https://doi.org/10.1039/c2cs15267c>
14. Wang S, Liu G, Wang L (2019) Crystal Facet Engineering of Photoelectrodes for Photoelectrochemical Water Splitting. *Chem Rev* 119:5192–5247. <https://doi.org/10.1021/acs.chemrev.8b00584>
15. Liu T, Vansaders B, Glotzer SC, Solomon MJ (2020) Effect of Defective Microstructure and Film Thickness on the Reflective Structural Color of Self-Assembled Colloidal Crystals. *ACS Appl Mater Interfaces* 12:9842–9850. <https://doi.org/10.1021/acsami.9b22913>
16. Kawamura A, Kohri M, Morimoto G, et al (2016) Full-Color Biomimetic Photonic Materials with Iridescent and Non-Iridescent Structural Colors. *Sci Rep* 6:1–10. <https://doi.org/10.1038/srep33984>

17. Yi B, Shen H (2017) Facile fabrication of crack-free photonic crystals with enhanced color contrast and low angle dependence. *J Mater Chem C* 5:8194–8200. <https://doi.org/10.1039/c7tc01549f>
18. Torres L, Margaronis A, Bellato Meinhardt BM, et al (2020) Rapid and Tunable Method to Fabricate Angle-Independent and Transferable Structurally Colored Films. *Langmuir* 36:1252–1257. <https://doi.org/10.1021/acs.langmuir.9b03516>
19. Fan W, Chen M, Yang S, Wu L (2015) Centrifugation-assisted Assembly of Colloidal Silica into Crack-Free and Transferrable Films with Tunable Crystalline Structures. *Sci Rep* 5:1–10. <https://doi.org/10.1038/srep12100>
20. Ge D, Yang X, Chen Z, et al (2017) Colloidal inks from bumpy colloidal nanoparticles for the assembly of ultrasmooth and uniform structural colors. *Nanoscale* 9:17357–17363. <https://doi.org/10.1039/c7nr06380f>
21. Takeoka Y, Yoshioka S, Takano A, et al (2013) Production of colored pigments with amorphous arrays of black and white Colloidal particles. *Angew Chemie - Int Ed* 52:7261–7265. <https://doi.org/10.1002/anie.201301321>
22. Kohri M, Nannichi Y, Taniguchi T, Kishikawa K (2015) Biomimetic non-iridescent structural color materials from polydopamine black particles that mimic melanin granules. *J Mater Chem C* 3:720–724. <https://doi.org/10.1039/c4tc02383h>
23. Ferrari B, Moreno R (2010) EPD kinetics: A review. *J Eur Ceram Soc* 30:1069–1078. <https://doi.org/10.1016/j.jeurceramsoc.2009.08.022>
24. Corni I, Ryan MP, Boccaccini AR (2008) Electrophoretic deposition: From traditional ceramics to nanotechnology. *J Eur Ceram Soc* 28:1353–1367. <https://doi.org/10.1016/j.jeurceramsoc.2007.12.011>
25. Katagiri K, Tanaka Y, Uemura K, et al (2017) Structural color coating films composed of an amorphous array of colloidal particles via electrophoretic deposition. *NPG Asia Mater* 9:e355. <https://doi.org/10.1038/am.2017.13>
26. Katagiri K, Uemura K, Uesugi R, et al (2018) Structurally colored coating films with tunable iridescence fabricated: Via cathodic electrophoretic deposition of silica particles. *RSC Adv* 8:10776–10784. <https://doi.org/10.1039/c8ra01215f>
27. Katagiri K, Uemura K, Uesugi R, et al (2020) Robust structurally colored coatings composed of colloidal arrays prepared by the cathodic electrophoretic deposition method with metal cation additives. *ACS Appl Mater Interfaces* 12:40768–40777. <https://doi.org/10.1021/acsami.0c10588>
28. Ammam M (2012) Electrophoretic deposition under modulated electric fields: A review. *RSC Adv* 2:7633–7646. <https://doi.org/10.1039/c2ra01342h>
29. Tran GTH, Koike M, Uchikoshi T, Fudouzi H (2020) Fabrication of polystyrene colloidal crystal film by electrophoretic deposition. *Adv Powder Technol* 31:3085–3092. <https://doi.org/10.1016/j.appt.2020.05.029>
30. Velev OD, Bhatt KH (2006) On-chip micromanipulation and assembly of colloidal particles by electric fields. *Soft Matter* 2:738–750. <https://doi.org/10.1039/b605052b>
31. Powers RW (1975) The Electrophoretic Forming of Beta-Alumina Ceramic. *J Electrochem Soc* 122:490–500. <https://doi.org/10.1149/1.2134246>
32. Van der Biest OO, Vandeperre LJ (1999) ELECTROPHORETIC DEPOSITION OF MATERIALS. *Annu Rev Mater Sci* 29:327–352. <https://doi.org/10.1146/annurev.matsci.29.1.327>
33. The Chemical Society of Japan (1984) *Handbook of Chemistry: Pure Chemistry.*, 3rd ed. Maruzen Publishing Co.,Ltd., Tokyo
34. Basu RN, Randall CA, Mayo MJ (2001) Fabrication of Dense Zirconia Electrolyte Films for Tubular Solid Oxide Fuel Cells by Electrophoretic Deposition. *J Am Ceram Soc* 84:33–40. <https://doi.org/10.1111/j.1151-2916.2001.tb00604.x>

35. Chen F, Liu M (2001) Preparation of yttria-stabilized zirconia (YSZ) films on La_{0.85}Sr_{0.15}MnO₃ (LSM) and LSM-YSZ substrates using an electrophoretic deposition (EPD) process. *J Eur Ceram Soc* 21:127–134. [https://doi.org/10.1016/S0955-2219\(00\)00195-3](https://doi.org/10.1016/S0955-2219(00)00195-3)
36. Aurenhammer F (1991) Voronoi diagrams—a survey of a fundamental geometric data structure. *ACM Comput Surv* 23:345–405. <https://doi.org/10.1145/116873.116880>
37. Nishida T, Sugihara K, Kimura M (2007) Stable marker-particle method for the Voronoi diagram in a flow field. *J Comput Appl Math* 202:377–391. <https://doi.org/10.1016/j.cam.2006.01.035>
38. Huerta A, Naumis GG, Wasan DT, et al (2004) Attraction-driven disorder in a hard-core colloidal monolayer. *J Chem Phys* 120:1506–1510. <https://doi.org/10.1063/1.1632893>
39. Kawamura A, Kohri M, Yoshioka S, et al (2017) Structural Color Tuning: Mixing Melanin-Like Particles with Different Diameters to Create Neutral Colors. *Langmuir* 33:3824–3830. <https://doi.org/10.1021/acs.langmuir.7b00707>
40. Takeoka Y, Yoshioka S, Takano A, et al (2013) Production of colored pigments with amorphous arrays of black and white Colloidal particles. *Angew Chemie - Int Ed* 52:7261–7265. <https://doi.org/10.1002/anie.201301321>
41. Scheid D, Lederle C, Vowinkel S, et al (2014) Redox- and mechano-chromic response of metallopolymer-based elastomeric colloidal crystal films. *J Mater Chem C* 2:2583–2590. <https://doi.org/10.1039/c3tc32525c>
42. Takeoka Y, Honda M, Seki T, et al (2009) Structural colored liquid membrane without angle dependence. *ACS Appl Mater Interfaces* 1:982–986. <https://doi.org/10.1021/am900074v>
43. Harun-Ur-Rashid M, Bin Imran A, Seki T, et al (2010) Angle-Independent Structural Color in Colloidal Amorphous Arrays. *ChemPhysChem* 11:579–583. <https://doi.org/10.1002/cphc.200900869>
44. Brown MA, Goel A, Abbas Z (2016) Effect of Electrolyte Concentration on the Stern Layer Thickness at a Charged Interface. *Angew Chemie - Int Ed* 55:3790–3794. <https://doi.org/10.1002/anie.201512025>
45. Neupane BB, Zhong Y, Wang G (2020) Study on self-assembly of colloidal particles at high ionic strength with stimulated emission depletion microscopy. *Eng Reports* 2:1–11. <https://doi.org/10.1002/eng2.12233>